Materials Letters 314 (2022) 131891

Contents lists available at ScienceDirect

Materials Letters

journal homepage: www.elsevier.com/locate/matlet

Core-shell structured Nb_2O_5@N-doped carbon nanoparticles as an anode material for Na-ion batteries

Yuvaraj Subramanian [a,b,*], Ganesh Kumar Veerasubramani [a], Myung-Soo Park [a], Dong-Won Kim [a,*]

[a] Department of Chemical Engineering, Hanyang University, Seoul 04763, Republic of Korea
[b] Department of Chemistry, University of Ulsan, Doowang-dong, Nam-gu, Ulsan, Republic of Korea

ARTICLE INFO

Keywords:
Nb_2O_5@N-doped carbon
Na-ion battery
Cycling stability

ABSTRACT

Core-shell structured Nb_2O_5@NC nanoparticles are successfully prepared by facile sonochemical approach using polyacrylonitrile as a carbon and nitrogen source. The prepared particles are in orthorhombic phase of T-Nb_2O_5 crystal structure and the particles exist in uniform spherical shape and size in the range of 60–80 nm. The Raman and XPS analysis confirms the presence of carbon and nitrogen in the prepared sample. The electrochemical performance demonstrates the good cycling stability of Nb_2O_5@NC electrode than pristine. Here, carbon aid to reduce the side reaction on the electrode/electrolyte interface and increase the electronic conductivity of the electrode thus leads to superior electrochemical performance.

1. Introduction

In the past decades, Li-ion batteries are widely investigated due to its high energy density. However, the less availability of lithium sources restricts the lithium ion battery in large scale applications. To tackle this problem, sodium-ion battery is considered as a promising candidate instead of LIBs, because sodium source is highly abundant in nature [1,2]. Recently, a lot of materials have been investigated as electrode material for sodium-ion batteries [2,3]. Among them, Nb_2O_5 material has been considered as a good intercalation based anode material for sodium ion battery due to its high power density through fast Na^+ ion insertion/extraction process [4–6]. Nevertheless, the Nb_2O_5 material has low electronic conductivity (3.4×10^{-6} S cm^{-1}) that impedes the high power density of the electrode [7]. To enhance the power density, the particle size is reduced to nano-level and carbon coating is necessary [8,9]. In which, nanoparticles offers the high reactive sites and fast ionic transport within the electrode material and carbon coating enhanced the electronic conductivity between the particles. These specified factors could facilitate to achieve a high electrochemical performance.

In the recent years, many groups investigated the Nb_2O_5 material for Li-ion and Na-ion batteries. Especially, Lee et al. reported Nb_2O_5@NC nanoparticles by using water-in-oil microemulsion method [5]. Yu et al. prepared the self-assembled Nb_2O_5 nanosheets through hydrothermal method for Na-ion battery application [6]. The above-mentioned process has disadvantages like, prolonging synthesis process and highly expensive solvent used for the synthesis. Interestingly, sonochemical synthesis is an effective approach that can producing the high intensity shockwaves that facilitate to rapid crystal growth, thereby resulting in uniform size and shape particles in a short time [10]. In this perspective, we prepared Nb_2O_5@NC nanoparticles by cost-effective and facile sonochemical approach. The prepared Nb_2O_5@NC nanoparticles offer the high reversible capacity and good cycling stability compared to pristine Nb_2O_5 nanoparticles.

2. Experimental details

In the first step, 6 mmol of Niobium ethoxide was dissolved in 80 mL of ethanol and the solution was kept into the ultrasonication chamber. Then, 2 mL of NH_4OH was added dropwise to the above solution followed by massive nanoparticles produced due to condensation and hydrolysis process, and sonication process was continued for 10 min. The obtained white color precipitate washed with water and ethanol, and then dried at 80 °C for 12 h, subsequently calcinated at 600 °C for 2 h to acquire Nb_2O_5 nanoparticles. Next, 0.6 g of polyacrylonitrile (PAN) dissolved into 5 mL of NMP solution. Then, 0.5 g of Nb_2O_5 nanoparticles was dispersed in PAN solution using ultrasonication. Subsequently, the above mixture was kept at 70 °C for 12 h under magnetic stirring. Finally, the mixture was transferred to vacuum oven at 120 °C for 12 h to

* Corresponding author at: Department of Chemical Engineering, Hanyang University, Seoul 04763, Republic of Korea.
E-mail addresses: yuvarajphysics@gmail.com (Y. Subramanian), dongwonkim@hanyang.ac.kr (D.-W. Kim).

https://doi.org/10.1016/j.matlet.2022.131891
Received 25 October 2021; Received in revised form 29 January 2022; Accepted 7 February 2022
Available online 10 February 2022

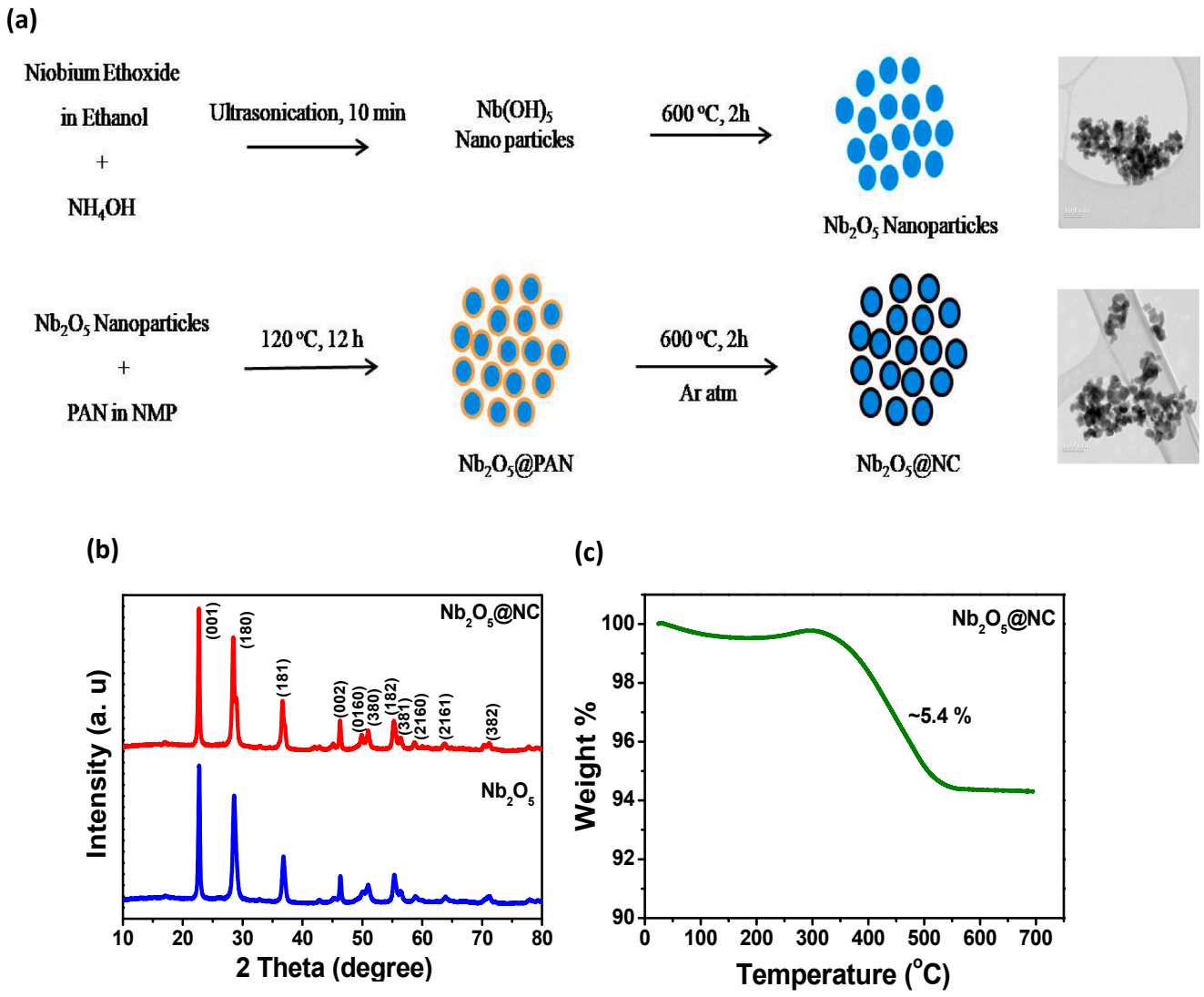

Fig. 1. (a) Synthesis process, (b) XRD pattern and (c) TGA curve of Nb_2O_5@NC.

remove the NMP solvent followed by calcinated at 600 °C for 2 h in Ar atmosphere to obtain Nb_2O_5@NC (Synthesis process simply shown in Fig. 1a).

The structural and morphology analysis were carried out using XRD (Rigaku Mini Flex X-ray diffractometer, Cu K_α radiation), TGA (SDT Q600, TA Instrument), Raman spectrum (NRS-3100, 532 nm excitation), XPS (VG multilab, ESCA system, 220i) and TEM (JEOL, JEM 2100F) techniques. The electrode material prepared by using 70:20:10 wt% of Nb_2O_5, Ketjen black and CMC binder which were uniformly mixed using water. The slurry was coated on the Cu foil and dried at 80 °C for 12 h under vacuum. The coin cell was assembled by using sodium as reference and glass fiber as separator. The separator was soaked with 1 M $NaClO_4$ in EC/PC (1:1) with 10 wt% of FEC. Charge-discharge analysis was conducted at galvanostatic conditions in the voltage range of 0.01 to 3.0 V using battery cycler (WBCS 3000, Wonatech). EIS carried out at 10 mHz-100 kHz with 10 mV amplitude.

3. Results and discussion

The synthesis process of Nb_2O_5 and Nb_2O_5@NC was simply shown in Fig. 1a. Fig. 1b shows the XRD pattern of Nb_2O_5 and Nb_2O_5@NC. All the diffraction peaks were well consistent with the orthorhombic phase of T-Nb_2O_5 with Pbam space group according to the standard XRD pattern (JCPDS: 30-0873). It obviously indicated that after carbon coating, the Nb_2O_5 nanoparticles exist in same phase without any detection of impurity phases. Moreover, the total amount of carbon and nitrogen present in the sample was around 5.4 %, which was deduced from the TGA analysis (Fig. 1c). Precisely, the carbon and nitrogen percentage was analyzed using CHNS analyzer and their weight percentage was 4.28 and 1.12 wt%, respectively.

Raman spectrum of Nb_2O_5@NC nanoparticles (Fig. 2a) showed the two vibrational modes at 261 and 637 cm^{-1}, associated with the Nb-O-Nb angle deformation and Nb-O-Nb bridging bond of distorted NbO_6 octahedra [11]. In addition, two strong peaks at 1349 and 1596 cm^{-1}, attributed to D and G-band of amorphous carbon [12]. The small peak at 986 cm^{-1} associated with the Nb=O bond on the surface of Nb_2O_5 particles not in the bulk [13]. XPS deconvoluted spectrum of Nb 3d region (Fig. 2b), it indicated the two binding energy at 206.8 and 209.5 eV corresponding to the Nb $3d_{5/2}$ and Nb $3d_{3/2}$ spectral line of Nb^{5+} [14]. The deconvoluted spectra of C 1s spectra (Fig. 2c) exhibited the two peaks located at 284.4 and 286.7 eV pertaining to the functional group of C–C and C–O [14]. The N 1s region in Fig. 2d, suggested that two peaks at 399.7 and 397.8 eV, attributed to the functional group of pyrrolic-N and pyridinic-N, respectively. The existence of nitrogen in the carbon could facilitate to enhance the electronic conductivity and charge transfer between the electrode and electrolyte interface [15].

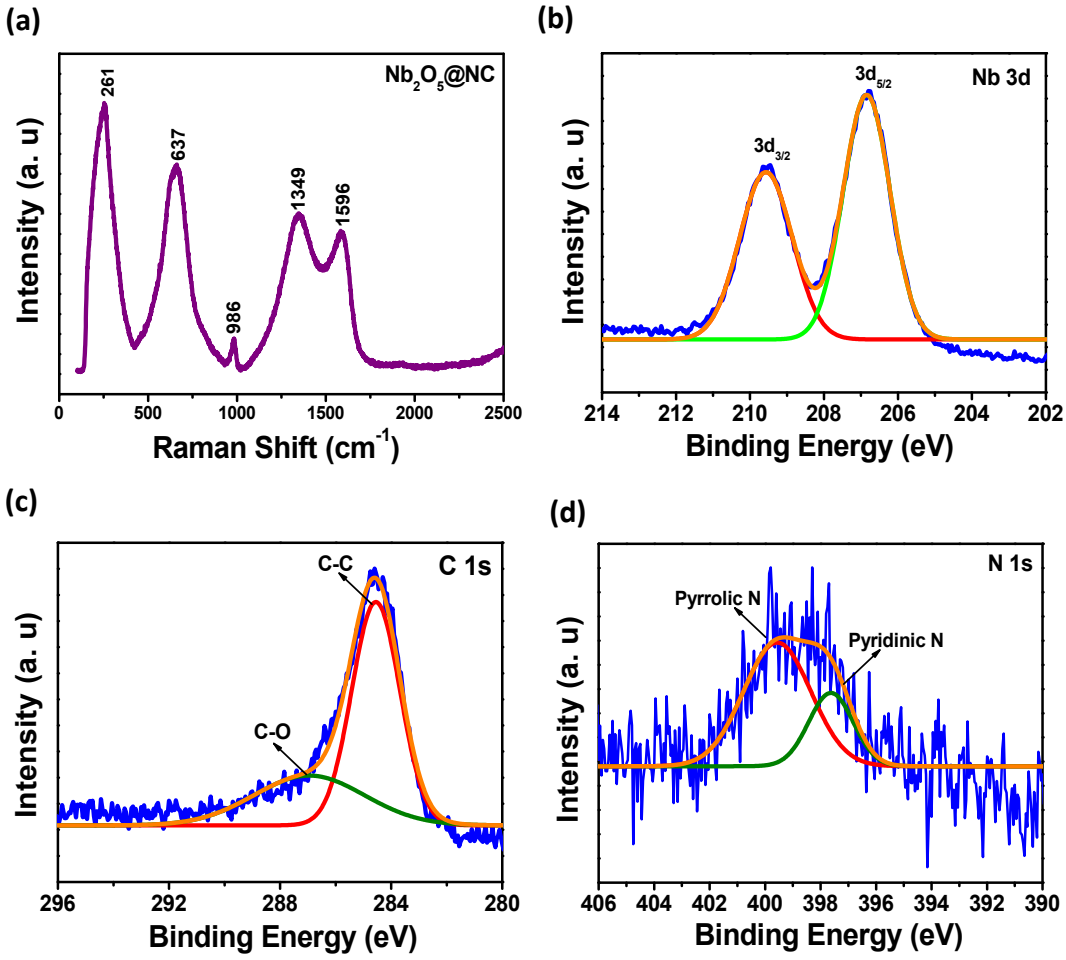

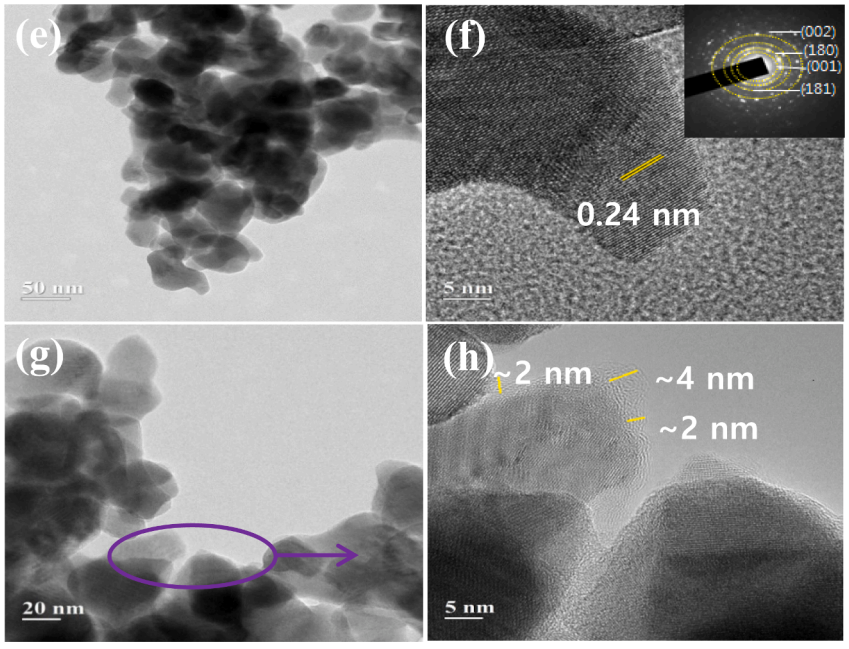

Fig. 2. (a) Raman spectrum and (b–d) XPS deconvolution spectrum of Nb_2O_5@NC, (e, g) TEM, and (f, h) HRTEM images of Nb_2O_5 and Nb_2O_5@NC.

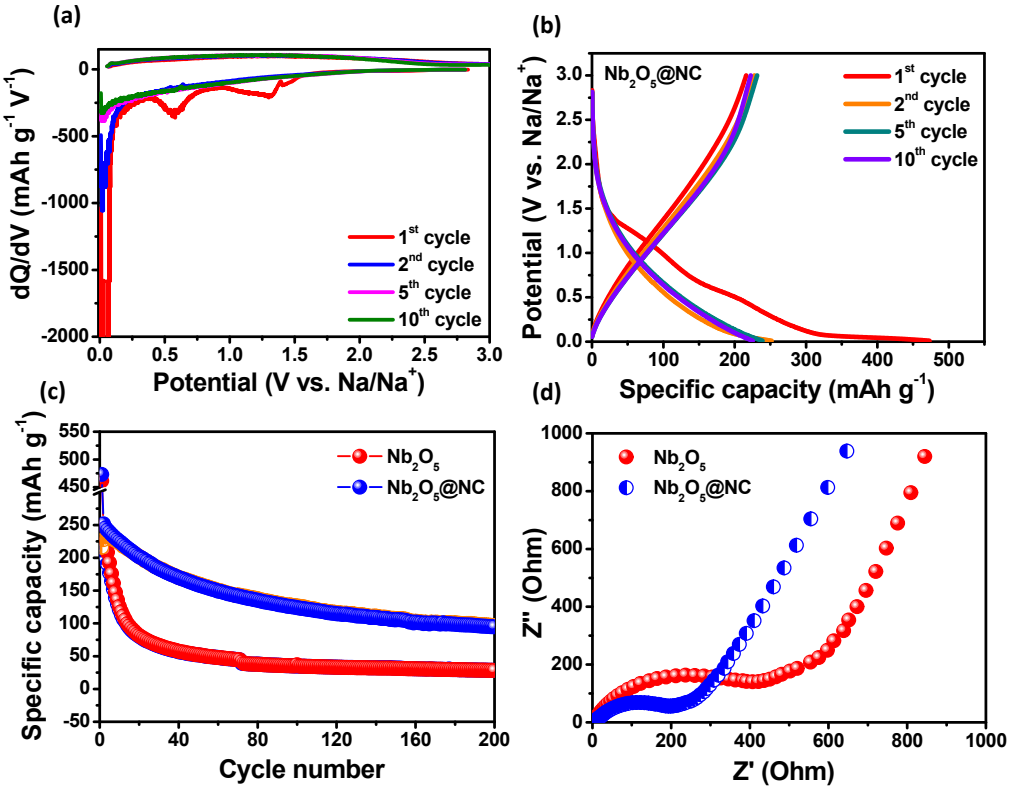

Fig. 3. (a, b) dQ/dV and charge-discharge curve of Nb_2O_5@C, and (c, d) Cycling stability and Nyquist plot of Nb_2O_5 and Nb_2O_5@C.

Fig. 2e shows the TEM image of pristine Nb_2O_5 sample that seems to be uniform sphere shape particles with size in the range of 60–80 nm. Fig. 2f clearly indicated the lattice spacing value of 0.24 nm that merely coincide with the (181) lattice plane of T-Nb_2O_5. The observed diffraction fringes (inset Fig. 2g) inferred the polycrystalline nature of Nb_2O_5 particles and their lattice spacing values were coincided with the lattice planes of T-Nb_2O_5. The TEM image of Nb_2O_5@NC shown in Fig. 2h, it obviously shows the very thin layer of carbon around 2–4 nm was encapsulated over the Nb_2O_5 nanoparticles.

The dQ/dV curve was carried out to identify the charge storage mechanism of Nb_2O_5@NC, in Fig. 3a. First sodiation process showed the multiple reduction peaks that associated with the electrolyte decomposition [7]. During anodic cycle, broad oxidation peak was observed and same trend followed on subsequent cycles. This behavior associated with the pseudocapacitive nature of Nb_2O_5 nanoparticles [16]. Fig. 3b, charge-discharge profile of Nb_2O_5@NC indicated one sloping curve without any plateau region that assures the continuous Na-ion insertion into the Nb_2O_5 crystal lattice. The cell demonstrated the initial discharge/charge capacity values were 473/216 mAh g^{-1} with 52.3% of coulombic efficiency. The high initial discharge capacity and low coulombic efficiency attributed to the electrolyte decomposition and side reaction with electrode and electrolyte interface. After the second cycle, the coulombic efficiency retain to 90.5% due to minimized decomposition of electrolyte. Fig. 3c demonstrates the discharge capacity over 200 cycles at 0.2 C that showed the linear drop in capacity on continuous cycles which is due to the unstable SEI layer formation. The discharge capacity was reached to 28 and 96 mAh g^{-1} after 200 cycles for Nb_2O_5 and Nb_2O_5@NC nanoparticles. Compared to pristine, the carbon coated Nb_2O_5 nanoparticles demonstrated the high discharge capacity and better cycling stability. Moreover, the Nb_2O_5@NC electrode demonstrated the better electrochemical performance than reported anode materials such as TiO_2 and $NaAlTi_3O_8$ [17,18]. The enhanced electrochemical performance of Nb_2O_5@NC was clarified using Nyquist plot after 200 cycles (Fig. 3d). The semicircle indicates that the Nb_2O_5@NC electrode exhibited the lower R_{ct} value compared to Nb_2O_5 because of carbon coating. Here, the carbon shell acts as an electronic conducting mediator that reduces the internal resistance between the active material and the current collector. The overall results assured that the carbon coating enhancing the electronic conductivity and maintained the structural stability of pristine Nb_2O_5 nanoparticles.

4. Conclusions

Nb_2O_5@NC particles were successfully prepared by two-step process and the prepared particles exist in nano-size around 60–80 nm with spherical shape. The electrochemical result deliberately shows the high reversible capacity and good cycling stability (95 mAh g^{-1}, 200 cycles) of Nb_2O_5@NC electrode compared to pristine. Also, the EIS analysis was suggesting that low R_{ct} value of Nb_2O_5@NC electrodes after cycling process. The overall results concluded that the carbon coating on Nb_2O_5 significantly enhancing the electronic conductivity and maintain the structural stability of pristine Nb_2O_5 nanoparticles.

CRediT authorship contribution statement

Yuvaraj Subramanian: Conceptualization, Methodology, Data curation, Writing – review & editing. **Ganesh Kumar Veerasubramani:** Formal analysis, Writing – review & editing. **Myung-Soo Park:** Formal analysis. **Dong-Won Kim:** Supervision, Writing – review & editing, Project administration, Funding acquisition.

Declaration of Competing Interest

The authors declare that they have no known competing financial interests or personal relationships that could have appeared to influence the work reported in this paper.

Acknowledgements

This work was supported by the National Research Foundation of Korea (NRF) funded by the Korea government (Ministry of Science, ICT and Future Planning) (2019R1A4A2001527 and 2021R1A2C2011050).

References

[1] H. Kim, H. Kim, Z. Ding, M.H. Lee, et al., Adv. Energy Mater. 6 (2016) 1600943.
[2] Y. Huang, Y. Zheng, X. Li, et al., ACS Energy. Lett. 3 (2018) 1604–1612.
[3] L.P. Wang, L. Yu, X. Wang, et al., J. Mater. Chem. A 3 (2015) 9353–9378.
[4] H. Kim, E. Lim, C. Jo, et al., Nano Energy 16 (2015) 62–70.
[5] E. Lim, C. Jo, M.S. Kim, M.-H. Kim, et al., Adv. Funct. Mater. 26 (2016) 3711.
[6] H. Li, Y. Zhu, S. Dong, L. Shen, et al., Chem. Mater. 28 (2016) 5753–5760.
[7] L. Kong, C. Zhang, S. Zhang, J. Wang, et al., J. Mater. Chem. A 2 (2014) 17962–17970.
[8] G.Q. Zou, H.S. Hou, Y. Zhang, et al., J. Electrochem. Soc. 163 (2016) A3117–A3125.
[9] S. Yuvaraj, K. Karthikeyan, et al., Electrochim. Acta 158 (2015) 446–456.
[10] S. Yuvaraj, R.K. Selvan, et al., Ultrason. Sonochem. 21 (2014) 599–605.
[11] E. Lim, C. Jo, H. Kim, M.-H. Kim, Y. Mun, et al., ACS Nano 9 (2015) 7497–7505.
[12] J. Lee, M.C. Orilall, S.C. Warren, et al., Nat. Mater. 7 (2008) 222–228.
[13] R.M. Pittman, A.T. Bell, J. Phys. Chem. 97 (1993) 12178–12185.
[14] T.T. Tung, M. Castro, T.Y. Kim, et al., J. Mater. Chem. 22 (2012) 21754–21766.
[15] L. Zhao, Y.S. Hu, H. Li, et al., Adv. Mater. 23 (2011) 1385.
[16] J. Yang, Z. Chen, H. Wang, et al., Mater. Lett. 207 (2017) 149–152.
[17] J.P. Huang, D.D. Yuan, H.Z. Zhang, et al., RSC Adv. 3 (2013) 12593–12597.
[18] X. Ma, K. An, J. Bai, et al., Sci. Rep. 7 (2017) 162.